On the Impact of the Fuel Dissolution Rate Upon Near-Field Releases From Nuclear Waste Disposal

António J. de C. Pereira
Department of Physics, Stockholm Center for Physics, Astronomy and Biotechnology, Stockholm University.
Roslagstullsbacken 21, 106 91 Stockholm, Sweden
antonio@fysikum.su.se

ABSTRACT

Calculations of the impact of the dissolution of spent nuclear fuel on the release from a damaged canister in a KBS-3 repository are presented. The dissolution of the fuel matrix is a complex process and the dissolution rate is known to be one of the most important parameters in performance assessment models of the near-field of a geological repository. A variability study has been made to estimate the uncertainties associated with the process of fuel dissolution. The model considered in this work is a 3D model of a KBS-3 copper canister. The nuclide used in the calculations is Cs-135. Our results confirm that the fuel degradation rate is an important parameter, however there are considerable uncertainties associated with the data and the conceptual models. Consequently, in the interests of safety one should reduce, as far as possible, the uncertainties coupled to fuel degradation.

1. INTRODUCTION

Estimation of the long-term impact of radionuclides on the biosphere and on man from a deep geological repository for spent nuclear fuel or high-level nuclear waste is a complicated task, owing to the uncertainties associated with many of the physical and chemical processes and to the huge time scales involved. Probabilistic calculations tend to be used to estimate the predictions of long-term releases that will impact on man and other biota. It is essential to support probabilistic modelling with deterministic calculations because the latter give us a deeper insight into the ongoing physical and chemical processes than do probabilistic simulations. In fact, probabilistic Monte Carlo calculations require the use of simplified models, fast enough to allow the thousands of simulations that are necessary to get good statistics for the analysis. Those simplified models (in general, 1D models) are not detailed enough to cope with coupled flow and physical- and chemical processes.

The aim of this work was to investigate the impact of the fuel degradation on the radionuclide release at the interface between the repository's near-field and the geosphere. The fuel dissolution is a complex chemical process and the laboratory data are affected by important uncertainties. We assumed that a fraction of the inventory in the interior of the canister is available for immediate migration, i.e. it is dissolved in water. This amount, the instant release fraction (IRF) is denoted by α. The IRF is nuclide specific and corresponds to gap- and grain boundary releases. The rest of the radionuclide inventory will be able to commence migration as a result of the gradual dissolution of the fuel matrix in which the nuclides are embedded (congruent dissolution). The fuel dissolution can be estimated by a

simple release model as in Hedin [1], assuming a degradation rate D_F that affects the $(1 - \alpha)$ fraction of the inventory. Following Hedin, the production rate $P(t)$ is given by:

$$P(t) = M_0 D_F(1-\alpha)\exp(-\lambda t)$$
$$t_{Delay} < t < t_{Delay} + D_F^{-1} \quad (1)$$

where:
M_0 is the inventory at time t_o (s)
D_F is the degradation rate for the fuel matrix (s^{-1})
α is the fraction of the waste that is immediately available for migration (and is dimensionless) and t_{Delay} is the time at which the canister starts leaking

To assess the impact uncertainties of the dissolution rate have on the release from the near-field, we use in this paper a near-field model which is an improved version of another three-dimensional model developed in previous work Pereira [2, 3]. The main difference between the two-models is the way in which some of the boundary conditions are treated in addition to which there is the explicit inclusion of a fracture crossing the canister deposition hole and of a disturbed zone, as explained later on.

2. MODEL GEOMETRY OF A REPOSITORY SECTION

2.1 MODEL DESCRIPTION

The model geometry describes a fuel canister, approximately 4.8 m high with an inner diameter equal of 0.95 m. We assume that the welded copper lid had initial but undetected damage, so that after three hundred years a fully developed corrosion channel (a small pinhole) connects the interior of the canister to the outside. This pinhole is a pathway with an assumed cross-section of 10^{-6} m^2 †. The pinhole is the pathway through which nuclides diffuse into the bentonite clay surrounding the canister. The diffusion gradient between the interior of the canister and the bentonite is controlled mainly by the fuel dissolution rate.

The repository is excavated in fractured granite (Figure 1). The nuclides that enter the bentonite buffer will be transported to the geosphere by groundwater circulating in the fractures adjacent to the buffer. Some short-lived nuclides will have time to decay completely and therefore will never reach the geosphere. Others will diffuse through the bentonite until they come into contact with the rock. In the model, we consider two horizontal rock fractures, one at the level of the corrosion pinhole and the other above it, at the level of the tunnel sole (Figure 1). These fractures are denominated Q1 and Q2 following the notation used by Hedin [1]. The Q2 fracture was introduced to represent the higher conductivity of the disturbed zone formed at the bottom of the tunnel as a result of the excavation process when building the repository. In our model we "collect" the nuclides at the outlet of these two fractures. The flux at the outlet represents therefore the amount of nuclides leaving the near-field and entering in the geosphere.

Iodine, Caesium and Chlorine are between the first elements to be released when water comes in contact with the fuel matrix. The ions I^-, Cs^+ and Cl^- form salts with high solubility in water and because a fraction of their inventory (the IRF fraction mentioned above) accumulates in the fuel-cladding gap and at grain boundaries, they are immediately

† In Hedin [1], the pinhole also has an initial cross-section of 10^{-6} m^2, but this increases suddenly at 20 000 years to 10^{-2} m^2. In this work we simulate only the first 10 000 years.

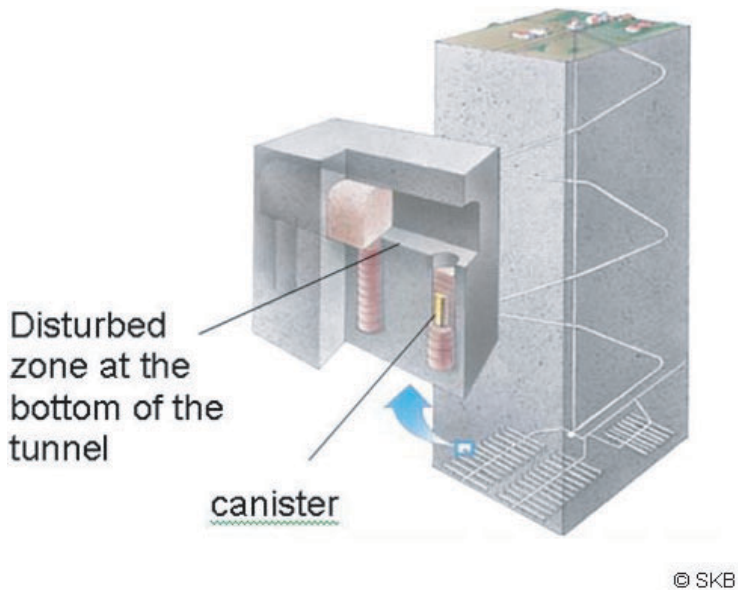

Figure 1 An overview of a section of the KBS-3 repository and its near field. The canister and the simulated disturbed zone at the bottom of the tunnel are indicated in the picture.

released. Radionuclide concentrations are controlled by the solubilities of the different elements under the near-field conditions. The concentrations of Iodine, Caesium and Chlorine are not solubility limited. We can therefore expect that the impact of fuel degradation may be higher for these nuclides. Caesium is a weakly-sorbing nuclide and it is the one that we use for our calculations.

3. NUMERICAL MODEL AND INPUT DATA

The geometry of a repository section, shown in Figure 2, uses the symmetry of the problem to reduce the computational load of our three-dimensional finite element model. However symmetries are not fully exploited here (for instance a 2D symmetry axial model could be used). The motivation for keeping the geometry of the model and using the actual shape is that we intend to use it in other studies addressing more realistic situations, such as how bentonite erosion can impact on the release rates. Bentonite erosion has been identified as one of the most serious potential threats for the long-term safety of a repository SKB [4].

The model consists of several sub-domains: the interior of the canister or the "source term" is denoted as domain Ω_1; the pinhole, domain Ω_2; the bentonite, domain Ω_3; the fracture Q1, domain Ω_4 and the fracture Q2, domain Ω_5.

The numerical model takes into account the main mass transport processes in the near-field. These are advection, diffusion, sorption, and radionuclide decay. The length of the fractures considered here is short, so that the diffusion from the fracture to the adjacent rock (matrix diffusion) is ignored. Sorption on the walls of the fractures is also ignored.

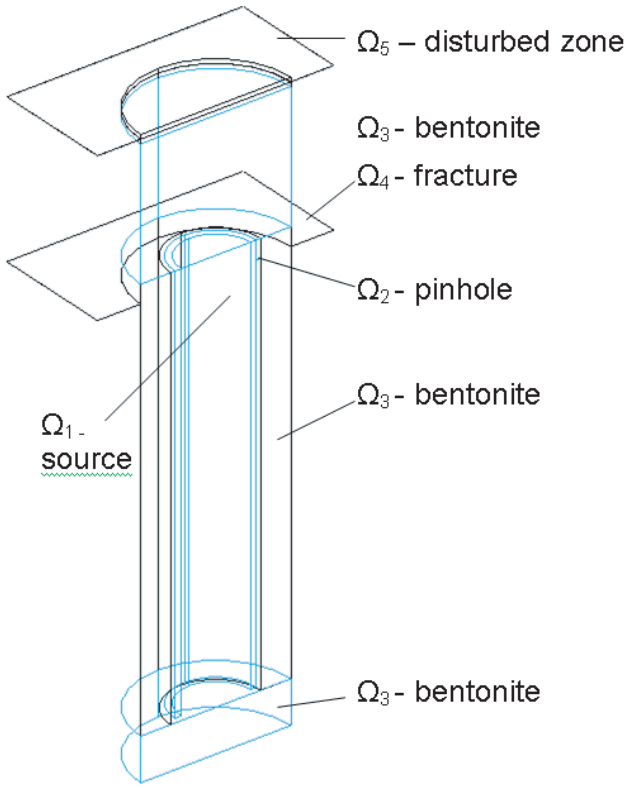

Figure 2 The geometry of the near-field.

3.1 THE SOURCE TERM

The mass transport within the canister (domain Ω_1) is described by a time-dependent diffusion equation that includes radionuclide decay and associated initial and boundary conditions:

$$\frac{\partial c(\mathbf{r},t)}{\partial t} + \nabla \cdot (-D\nabla \cdot c(\mathbf{r},t)) = -\lambda c(\mathbf{r},t) \qquad \text{in} \quad \Omega_1 \tag{1a}$$

$$c(\mathbf{r},0) = c_0(\mathbf{r}) \tag{1b}$$

$$-\mathbf{n} \cdot (-D\nabla c) = 0 \tag{1c}$$

where
c ($\mathbf{r}$,t) is the nuclide concentration in the domain Ω_1 (mol m^{-3}),
c_0 is the initial nuclide concentration in the domain Ω_1 (mol m^{-3}),
D is the diffusivity of the water (m^2 s^{-1}),
λ is the radioactive decay constant (s^{-1}) and
α is the instant release fraction (dimensionless)

3.2 THE PINHOLE

The transport through the pinhole (Ω_2 domain) is also given by the time-dependent three-dimensional diffusion equation and the relevant associated initial and boundary conditions:

$$\frac{\partial c(\mathbf{r},t)}{\partial t} + \nabla \cdot (-D\nabla \cdot c(\mathbf{r},t)) = -\lambda c(\mathbf{r},t) \qquad \text{in} \quad \Omega_2 \tag{2a}$$

$$c(\mathbf{r},0) = c_0(\mathbf{r}) \tag{2b}$$

$$-\mathbf{n} \cdot (-D\nabla c) = 0 \tag{2c}$$

where
c ($\mathbf{r}$,t) is the nuclide concentration in the domain Ω_2 (mol m^{-3}),
c(0), the initial nuclide concentration in the domain Ω_2, is nil (mol m^{-3}),
D is the water diffusivity (m^2 s^{-1}) and
λ is the radioactive decay constant (s^{-1}).

Eqn. (2c) encapsulates the insulating boundary conditions at relevant surfaces of the domain. The inlet and the outlet of the pinhole are interior boundaries. We assume that the pinhole is entirely filled with water.

3.3 THE BENTONITE

As long as the bentonite is intact (no occurrence of erosion), the advective water flow is extremely low and therefore we describe the mass transport in the bentonite (Ω_3 -domain) by a time-dependent diffusion-reaction equation that also includes radionuclide decay:

$$R_i \frac{\partial c_i(\mathbf{r},t)}{\partial t} + \nabla \cdot (-D_i \nabla \cdot c_i(\mathbf{r},t)) = -\lambda_i c_i(\mathbf{r},t) \qquad \text{in} \quad \Omega_3 \tag{3a}$$

$$c(\mathbf{r},0) = c_0(\mathbf{r}) \tag{3b}$$

$$-\mathbf{n} \cdot (-D\nabla c) = 0 \tag{3c}$$

where,
c_i($\mathbf{r}$,t) is the concentration of nuclide i, in the domain Ω_3, (mol m^{-3}),
c_i(0), the initial nuclide concentration in the domain Ω_3, is nil (mol m^{-3}),
R_i is the retardation coefficient of nuclide i and is dimensionless,
D_i is the diffusion coefficient of nuclide i (m^2 s^{-1}) and
λ_i - is the radioactive decay constant of nuclide i (s^{-1}).

The retardation coefficient R_i is given by ε+ρ K_d where ε is the porosity, ρ the density and K_d the sorption coefficient.

3.4 THE FRACTURE Q1 AND THE DISTURBED ZONE Q2

The migration of radionuclides in the fracture Q1 and the disturbed zone Q2 (domains Ω_4 and Ω_5, respectively) is described by coupling the advective flow in the fractures to the mass transport. To compute the advective velocity $\mathbf{u}$ of the groundwater in the fractures, we solve the three-dimensional steady state Navier-Stokes' equation under the assumption of fluid incompressibility, eq. (4a), together with the continuity equation, eq. (4b):

$$\rho\, \mathbf{u} \cdot \nabla \mathbf{u} = -\nabla p + \eta \nabla^2 \mathbf{u} \tag{4a}$$

$$\nabla \cdot \mathbf{u} = 0 \tag{4b}$$

where:
u is the advective velocity in the fracture Q1 and the disturbed zone Q2 (m s^{-1}),
p is the pressure (N m^{-2}),
ρ is the water density (kg m^{-3}) and
η is the viscosity of water (N s m^{-2}).

Eq. (4a) is valid for a Newtonian fluid in the steady state. The gradient ∇_p has been chosen so that it conforms with the value of the Darcy velocity given by Hedin for a fracture in the near-field, Hedin [1]. The mass transport in the fracture Q1 and the disturbed zone Q2 is described by the time-dependent three-dimensional advection-diffusion-reaction equation, eq. (4c), to which the radionuclide decay has been added.

The advective velocity **u** couples the Navier-Stokes' and continuity equations, eqs. (4a and 4b) to the mass transport equation, eq. (4c):

$$R_i \frac{\partial c_i(\mathbf{r},t)}{\partial t} + \nabla \cdot (-D_i \nabla \cdot c_i(\mathbf{r},t)) = -\lambda_i c_i(\mathbf{r},t) - \mathbf{u}_i \cdot \nabla c_i(\mathbf{r},t) \tag{4c}$$

where,
$c_i(\mathbf{r},t)$ is the nuclide concentration in the domains Ω_4 and Ω_5 (mol m^{-3}),
R_i is the retardation coefficient and is dimensionless,
D_i is the diffusion coefficient (m^2 s^{-1}),
$\mathbf{u}_i$ is the advective velocity in the fracture Q1 and the disturbed zone Q2 (m s^{-1}) and
λ_i is the radioactive decay constant (s^{-1}).

The impact of the fuel dissolution rate has been studied using the caesium-135 nuclide as mentioned earlier. The nuclide-specific data is presented in Table1. It includes the half-life, the initial inventory M_0, the instantaneous release fraction α, the effective diffusivity in bentonite and the sorption coefficient, D_{eff}^{Bent} and K_d^{Bent} respectively. Two values for the instantaneous release fraction α were used: the first one has been taken from Hedin [1] and the other is simply twice this value. The nuclide considered here has infinite solubility.

Table II presents the non-nuclide-specific data, namely, the effective diffusivity of water D_e^{water}, the bentonite density ρ_{buff}, the bentonite porosity ε_{buff}, the fracture apertures b_{Q1} and b_{Q2}, the pinhole cross-section A_{Hole}, the pinhole length L_{Hole} and the degradation rate of the fuel matrix D_F. The degradation rate of the fuel matrix covers an uncertainty of two orders of magnitude.

The time at which the canister starts leaching, t_{delay} is taken to be 300 *years*.

Part of the input data set is a subset of the data used by Hedin [1]. Six case variations have been carried out for the two nuclides using three different rates for the fuel dissolution rate and two values for the IRF fraction. Table 3 displays the six combinations used:

Table 1: Nuclide-specific data

	Half-life	M_0	α	D_{eff}^{Bent}	K_d^{Bent}
Units	(years)	(Bq/canister)	(-)	(m^2/years)	(m^3/kg)
^{135}Cs	2.3×10^6	4.4×10^{10}	0.03, 0.06	1.9×10^{-2}	0.05

Table 2: Generic data

Parameter		Units	Value
Effective diffusivity of water	D_e^{water}	m^2 $years^{-1}$	3.2×10^{-2}
Density of bentonite	ρ_{buff}	kg m^{-3}	1600
Porosity of bentonite	ε_{buff}	-	0.41
Fracture apertures	b_{Q1} b_{Q2}	m	1×10^{-4}
Pinhole cross-section	A_{Hole}	m^2	1×10^{-6}
Pinhole length	L_{Hole}	m	0.05
Degradation rate of fuel matrix	D_F	$years^{-1}$	10^{-8}, 10^{-7}, 10^{-6}

Table 3: Case studies

	Nuclide	α	D_F (yr^{-1})
Case 1	^{135}Cs	0.03	10^{-6}
Case 2	^{135}Cs	0.03	10^{-7}
Case 3	^{135}Cs	0.03	10^{-8}
Case 4	^{135}Cs	0.06	10^{-6}
Case 5	^{135}Cs	0.06	10^{-7}
Case 6	^{135}Cs	0.06	10^{-8}

4. RESULTS AND DISCUSSION

The estimation of the radionuclide releases has been performed for a fracture density corresponding to one fracture per canister. Note that the pathway Q2 is treated as a fracture, but represents a damaged zone with higher conductivity that the rest of the tunnel and is not, therefore, included in the estimation of the fracture density for the deposition holes.

How the mesh used by the FEM- model could impact on convergence of the computed results was examined by using different meshes, and Table 4 shows some statistics for these meshes. The calculations were repeated for higher number of mesh points and it is conclude that numerical convergence is not affected by the grid used.

Table 4: Mesh statistics of the different domains

	Bentonite -upper block	Bentonite – lower block	Bentonite around the canister	Pinhole	Source term	Fracture	Disturbed zone
Type of mesh	Prismatic	Prismatic	Hexahedral	Hexahedral	Hexahedral	Hexahedral	Tetrahedral
Number of elements	5715	1905	4800	2400	2400	496	8470

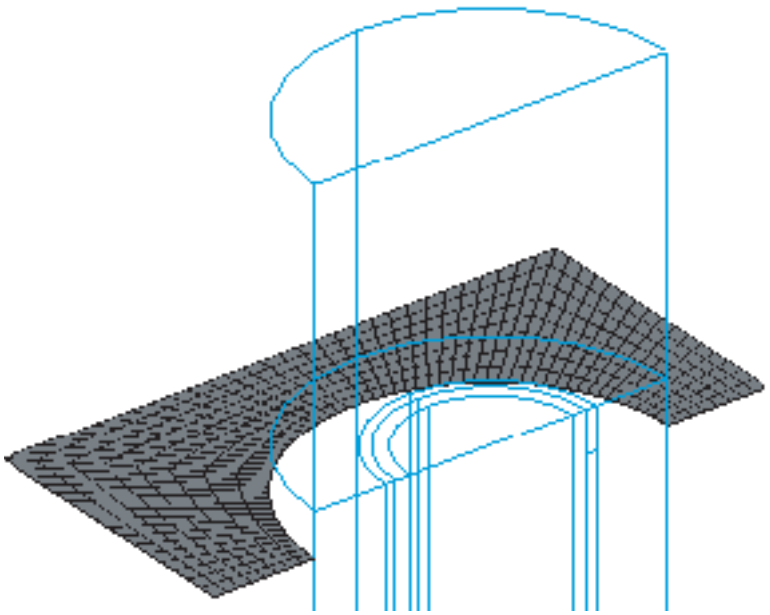

Figure 3. The hexahedral mesh taken for the Q1 fracture.

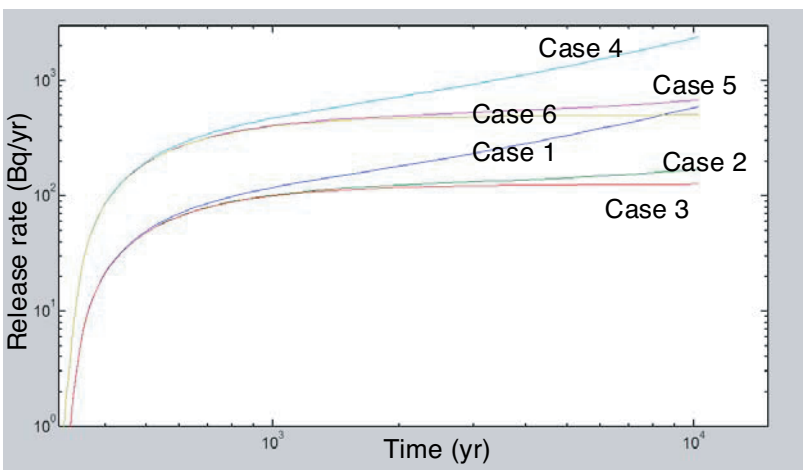

Figure 4 Breakthrough curves for the six cases modeled.

Figure 3 displays the hexahedral grid used in fracture Q1.

Figure 4 shows the breakthrough curves for the six cases simulated. The input data in Case 3 correspond to the parameters that Hedin used in his analytic model. Hedin developed his model to speed up Monte Carlo calculations for risk analyses. Our 3D model and Hedin's model are conceptually close to one another although Hedin used the resistance approach to mass transfer introduced in the earlier work of Neretnieks [5]. Given this similarity, we would expect to obtain a similar breakthrough curve for Case 3 to that of Hedin, which is in fact the case.

It is observed that cases 2 and 3 (for α equal to 0.03) and cases 5 and 6 (for α equal to 0.06) are relatively tight at 10 000 years. There is a significant jump, however, when the dissolution rate D_F increases by one order of magnitude from 10^{-7} to 10^{-6} for the same IRF (Cases 1 and 2, respectively Cases 4 and 5). At 10 000 years, the cases can be ordered by increasing order of importance as:

Case 3 < Case 2 < Case 6 < Case 1 < Case 5 < Case 4

The breakthrough curve corresponding to Case 1 increases more rapidly than that of Case 6 curve, making Case 1 the third most important case at 10 000 years. However the continued increase for Cases 1 and 4 over the later time period is considerably greater than that of the other four cases, enabling one to conclude that the parameter D_F is of paramount importance if the nuclide has a half-life that is not short and therefore we need to increase our understanding of uncertainties coupled to fuel degradation of nuclear fuels.

REFERENCES

[1] Hedin, A., Integrated Analytic Radionuclide Transport Model for a Spent Nuclear Fuel Repository in Saturated Fractured Rock. *Nuclear Technology*, (2002), 138, 79–205.

[2] Pereira, A., *Three Dimensional Modelling of a KBS-3 Canister for Spent Nuclear Fuel – phase II)*, (2007), SKI Report 2007:34.

[3] Pereira, A., A Three Dimensional Model of radionuclide migration from a canister of spent nuclear fuel. *Int. Jnl. of Multiphysics*, (2007), Vol. 1, nr. 2, 189–198.

[4] SKB TR-07-12. *RD&D Programme 2007. Programme for research, development and demonstration of methods for the management and disposal of nuclear waste*. Svensk Kärnbränslehantering AB, 2007.

[5] Neretnieks I. Stationary Transport of Dissolved Species in the Backfill Surrounding a Waste Canister in Fissured Rock: Some Simple Analytical Solutions. *Nuclear Technol*., 1986, 72, 196.